International Immunology, Vol. 30, No. 10, pp. 471–481
doi:10.1093/intimm/dxy046
Advance Access publication 16 July 2018

FEATURED ARTICLE

Immunological association of inducible bronchus-associated lymphoid tissue organogenesis in Ag85B-rHPIV2 vaccine-induced anti-tuberculosis mucosal immune responses in mice

Takahiro Nagatake[1], Hidehiko Suzuki[1], So-ichiro Hirata[1,2], Naomi Matsumoto[1], Yasuko Wada[1,3], Sakiko Morimoto[1], Ayaka Nasu[1], Michiko Shimojou[1], Mitsuo Kawano[4], Kentaro Ogami[5], Yusuke Tsujimura[5], Etsushi Kuroda[6,7], Norifumi Iijima[6,7], Koji Hosomi[1], Ken J. Ishii[6,7], Tetsuya Nosaka[4], Yasuhiro Yasutomi[5] and **Jun Kunisawa[1,2,3,8,9]**

[1]Laboratory of Vaccine Materials, Center for Vaccine and Adjuvant Research, and Laboratory of Gut Environmental System, National Institutes of Biomedical Innovation, Health and Nutrition (NIBIOHN), 7-6-8 Asagi Saito, Ibaraki, Osaka 567-0085, Japan
[2]Department of Microbiology and Immunology, Kobe University Graduate School of Medicine, 7-5-1 Kusunoki-cho, Chuo-ku, Kobe, Hyogo 650-0017, Japan
[3]Graduate School of Pharmaceutical Sciences, Osaka University, 1-1 Yamadaoka, Suita, Osaka 565-0871, Japan
[4]Department of Microbiology and Molecular Genetics, Mie University Graduate School of Medicine, 2-174 Edobashi, Tsu, Mie 514-8507, Japan
[5]Laboratory of Immunoregulation and Vaccine Research, Tsukuba Primate Research Center, NIBIOHN, 1-1 Hachimandai, Tsukuba, Ibaraki 305-0843, Japan
[6]Laboratory of Vaccine Science, WPI Immunology Frontier Research Center, Osaka University, Osaka 565-0871, Japan
[7]Laboratory of Adjuvant Innovation, Center for Vaccine and Adjuvant Research, NIBIOHN, 7-6-8 Asagi Saito, Ibaraki, Osaka 567-0085, Japan
[8]Division of Mucosal Immunology, Department of Microbiology and Immunology and International Research and Development Center for Mucosal Vaccines, The Institute of Medical Science, The University of Tokyo, 4-6-1 Shirokanedai, Minato-ku, Tokyo 108-8639, Japan
[9]Graduate School of Medicine, Graduate School of Dentistry, Osaka University, 1-1 Yamadaoka, Suita, Osaka 565-0871, Japan

Correspondence to: J. Kunisawa; E-mail: kunisawa@nibiohn.go.jp

Received 31 January 2018, *editorial decision* 5 July 2018; *accepted* 12 July 2018

Abstract

We previously reported that Ag85B-expressing human parainfluenza type 2 virus (Ag85B-rHPIV2) was effective as a nasal vaccine against tuberculosis in mice; however, the mechanism by which it induces an immune response remains to be investigated. In the present study, we found that organogenesis of inducible bronchus-associated lymphoid tissue (iBALT) played a role in the induction of antigen-specific T cells and IgA antibody responses in the lung of mice intra-nasally administered Ag85B-rHPIV2. We found that expression of Ag85B was dispensable for the development of iBALT, suggesting that HPIV2 acted as an iBALT-inducing vector. When iBALT organogenesis was disrupted in Ag85B-rHPIV2-immunized mice, either by neutralization of the lymphotoxin pathway or depletion of CD11b$^+$ cells, Ag85B-specific immune responses (i.e. IFN γ-producing T cells and IgA antibody) were diminished in the lung. Furthermore, we found that immunization with Ag85B-rHPIV2 induced neutrophil and eosinophil infiltration temporally after the immunization in the lung. Thus, our results show that iBALT organogenesis contributes to the induction of antigen-specific immune responses by Ag85B-rHPIV2 and that Ag85B-rHPIV2 provokes its immune responses without inducing long-lasting inflammation.

Keywords: iBALT, mucosa-associated lymphoid tissue, mucosal immunity, nasal vaccine, tertiary lymphoid organ

Introduction

Mucosa-associated lymphoid tissue (MALT) develops at the mucosal surface at various sites in the body such as the tear duct, respiratory tract and intestine, and this tissue provides a specialized environment for the initiation of antigen-specific immune responses (1, 2). Luminal antigens are taken up by MALT-associated M cells and transported to dendritic cells (DCs) for antigen processing and presentation, which leads to the expansion of antigen-specific T cells and the development of germinal centers as sites for immunoglobulin class-switch recombination and hypersomatic mutation (1, 2). MALT is categorized as a secondary lymphoid organ and therefore its development is programmed in ontogeny (1, 2). However, MALT is absent in the lung (3). Instead, inducible bronchus-associated lymphoid tissue (iBALT), a tertiary lymphoid organ, develops in the lung in response to infection by influenza (4) or vaccinia virus (5); inflammation induced by lipopolysaccharides (6), fine particles (7) or cigarette smoke (8); or diseases such as asthma (9–11) or chronic obstructive pulmonary disease (12). iBALT plays an important role in the induction of respiratory immune responses. Indeed, immune responses originating from iBALT are sufficient to clear influenza virus (4). It has also been shown that iBALT is induced by intra-nasal administration of replication-deficient Modified Vaccinia Ankara, which is widely used as a recombinant vaccine vector (5).

iBALT organogenesis does not require the transcriptional regulators Id2 and RORγt, which are essential for the differentiation of lymphoid tissue inducer cells and organogenesis of peripheral lymph nodes and Peyer's patches (6, 13–15). Therefore, iBALT organogenesis occurs independent of conventional lymphoid tissue inducer cells, which is a scenario similar to that of tear duct-associated lymphoid tissue and omental milky spots (1, 6, 16). Our group recently reported that alveolar macrophages function as iBALT inducer cells by producing IL-1α in response to inoculation with fine particles (7). It has also been reported that T helper (T_h) 17 cells initiate iBALT organogenesis by producing IL-17, which induces the expression of CXCL13 in response to lipopolysaccharide inoculation (6). Homeostatic chemokines such as CCL19, CCL21 and CXCL13 contribute to the development of iBALT in response to influenza virus infection (17). $CD11b^+CD11c^+$ DCs are reported to induce iBALT organogenesis by producing lymphotoxin and homeostatic chemokines in response to influenza or vaccinia virus infection (5, 18). In contrast, $CCR7^+$ T_{reg} cells are reported to suppress the development of iBALT (19). iBALT is equipped with immunocompetent cells such as T and B cells as well as DCs that form a highly organized lymphoid structure and are involved in the induction of antigen-specific immune responses to infection and allergy (4, 7, 10).

Mycobacterium bovis bacilli Calmette–Guerin (BCG) is the only currently licensed tuberculosis vaccine, but it is ineffective against adult pulmonary tuberculosis (20–22). BCG vaccine is administered subcutaneously and induces systemic immune responses; however, it does not induce immune responses in mucosal compartments, such as the respiratory mucosa. Therefore, the lack of efficacy of BCG vaccination in adults might be due to a lack of induction of antigen-specific immune responses in the respiratory mucosa. Recombinant viral vector vaccines have the potential to overcome this limitation because they induce respiratory immune responses (5).

Human parainfluenza type 2 virus (HPIV2; family Paramyxoviridae, genus *Rubulavirus*) possesses a single-strand, non-segmented, negative-stranded RNA genome. Ag85B is a major secretory protein that is involved in the synthesis of cell wall mycolic acid in mycobacteria (23). Our group recently developed Ag85B-expressing HPIV2 (Ag85B-rHPIV2) as a nasal vaccine against tuberculosis (24). Nasal immunization of mice with Ag85B-rHPIV2 induced a mucosal antigen-specific immune response in the lung and efficiently eliminated a pathogenic tuberculosis strain (24). However, the mechanisms underlying the immune response induced by Ag85B-rHPIV2 remain to be investigated. In the present study, we examined the role of iBALT in the immune response induced by Ag85B-rHPIV2 in mice. We also evaluated the safety of intra-nasal administration of Ag85B-rHPIV2 in mice by assessing inflammatory cell infiltration to the lung.

Methods

Animals

C57BL/6 wild-type mice (age, 6–8 weeks) were purchased from Japan SLC (Hamamatsu, Japan) and kept for at least 1 week before the start of the experiments in the specific pathogen-free animal facility at the National Institutes of Biomedical Innovation, Health, and Nutrition (NIBIOHN; Osaka, Japan). CD11b-diphtheria toxin receptor (DTR) transgenic mice were purchased from Jackson Laboratory (Bar Harbor, ME, USA). All experiments were conducted in accordance with the guidelines of the Animal Care and Use Committee of NIBIOHN and the Committee on the Ethics of Animal Experiments of NIBIOHN (DS25-2, DS25-3, DS27-47, DS27-48, DNA-395 and DNA-435).

Immunization with Ag85B-rHPIV2

Immunization was conducted as described previously with modifications (24). Briefly, adult mice were intra-nasally immunized with Ag85B-rHPIV2 (1×10^8 50% tissue culture infective dose/mouse; 50 μl volume) under anesthesia with pentobarbital, four times at 2-week intervals (i.e., on days 0, 14, 28 and 42), and then analyzed on day 56. In some experiments, immunized mice were additionally intra-peritoneally injected with lymphotoxin β receptor (LTβR)-Fc fusion protein (200 μg per mouse) on days –3, 7, 21, 35 and 49 to neutralize lymphotoxin-mediated signals (18, 25). In some experiments, immunized CD11b-DTR transgenic mice were additionally administered diphtheria toxin (50 ng intra-nasally per mouse and 500 ng intra-peritoneally per mouse) on days 7, 21, 35 and 49 to deplete $CD11b^+$ cells (26).

Administration with null-HPIV2

Administration with null-HPIV2 was conducted as described previously with modifications (18). Briefly, adult mice were intra-nasally administered null-HPIV2 (1×10^8 50% tissue culture infective dose per mouse; 50 μl volume) under anesthesia with pentobarbital, two times (days 0 and 7) and then analyzed on day 24.

Preparation of Ag85B-rHPIV2

Ag85B-rHPIV2 was generated as previously described, except for the intact M gene sequence in this study (Supplementary Figure 1) (27). Virus titers were determined by means of a cytopathic effect assay using Vero cells, and the results were expressed as 50% tissue culture infective dose values.

Preparation of LTβR-Fc fusion protein

LTβR-Fc-encoding plasmid was kindly provided by Dr C.F. Ware (Sanford Burnham Prebys Medical Discovery Institute, La Jolla, CA, USA) (25). Expi293 cells (Thermo Fisher Scientific, Waltham, MA, USA) were cultured in Expi293 Expression Medium (Thermo Fisher Scientific) in a 10% CO_2 atmosphere at 37°C with shaking. The mixture of LTβR-Fc-encoding plasmid and Lipofectamine 2000 (Thermo Fisher Scientific) and Opti-MEM (Thermo Fisher Scientific) was incubated at room temperature for 20 min. We then added the prepared transfection mixture to the Expi293 cells, and the cells were incubated in a 10% CO_2 atmosphere at 37°C without shaking. Supernatant was collected on days 7 and 14. After concentration by using an Amicon Ultra centrifugal filter (Merck Millipore, Darmstadt, Germany), LTβR-Fc fusion protein was purified by using a Protein G purification kit (Protein Ark, Sheffield, UK). Endotoxin was removed by using an endotoxin removal kit (Protein Ark). The solvent was exchanged with phosphate-buffered saline (PBS) by using a PD-10 column (GE Healthcare, Little Chalfont, UK).

Immunohistochemical analysis

Frozen tissue of the left lung was analyzed histologically as described previously with modifications (28). Tissue samples were washed with PBS (Nacalai Tesque, Kyoto, Japan) on ice and frozen in Tissue-Tek OCT compound (Sakura Finetek, Tokyo, Japan) in liquid nitrogen. Frozen tissue sections (6 μm) were prepared by using a CM3050 S cryostat (Leica Biosystems, Wetzlar, Germany) and were fixed for 30 min at 4°C in prechilled 95% ethanol (Nacalai Tesque) followed by 1 min at room temperature in prechilled 100% acetone (Nacalai Tesque). Tissue sections were washed with PBS for 10 min and then blocked in 2% (vol/vol) newborn calf serum in PBS for 30 min at room temperature in an incubation chamber (Cosmo Bio, Tokyo, Japan). Tissue sections were incubated with primary antibodies in 2% (vol/vol) newborn calf serum in PBS for 16 h at 4°C in the incubation chamber, washed once in 0.1% (vol/vol) Tween-20 (Nacalai Tesque) in PBS and then in PBS only (5 min each wash), and then stained with secondary antibodies in 2% (vol/vol) newborn calf serum in PBS for 30 min at room temperature in the incubation chamber. To visualize nuclei, tissue sections were washed twice (5 min each wash) with PBS and stained with DAPI (4′,6-diamidino-2-phenylindole; AAT Bioquest, Sunnyvale, CA, USA; 1 μM) for 10 min at room temperature in the incubation chamber. Finally, tissue sections were washed twice with PBS, mounted in Fluoromount (Diagnostic BioSystems, Pleasanton, CA, USA) and examined under a fluorescence microscope (BZ-9000; Keyence, Osaka, Japan). The following monoclonal antibodies and reagents were used for immunohistological analysis: purified anti-B220 (BioLegend, San Diego, CA, USA; 103202; 1:100), purified anti-CD3ε (BioLegend; 100302; 1:100), purified anti-CD11b (BioLegend; 101202; 1:100), purified anti-CD11c (BioLegend; 117302; 1:50), biotin–peanut agglutinin (PNA) (Vector Laboratories, Burlingame, CA, USA; B-1075; 1:100), AF488–anti-rat IgG (Thermo Fisher Scientific; A-11006; 1:200), Cy3–anti-Armenian hamster IgG (Jackson ImmunoResearch Laboratories, West Grove, PA, USA; 127-165-160; 1:200) and AF546–streptavidin (Thermo Fisher Scientific; S11225; 1:200). Cell nuclei were visualized by staining with DAPI as described above.

Cell isolation and flow cytometric analysis

Cell isolation and flow cytometry were performed as described previously with modifications (28). The right lung was cut into small pieces by using scissors and then incubated twice in 0.5 mg ml^{-1} collagenase (Wako, Tokyo, Japan) in RPMI-1640 medium (Sigma-Aldrich, St. Louis, MO, USA) containing 2% (vol/vol) newborn calf serum (Equitech-Bio, Kerrville, TX, USA) for 15 min at 37°C with stirring. The cell suspensions were then filtered through cell strainers (pore size, 70 μm; BD Biosciences, Franklin Lakes, NJ, USA).

For cell surface staining, cell samples were first incubated with an anti-CD16/32 monoclonal antibody (TruStain FcX; BioLegend; 101320; 1:100) to avoid non-specific staining, and then stained with the following fluorescently labeled monoclonal antibodies: phycoerythrin–anti-B220 (BioLegend; 103208; 1:100), AF647–anti-GL7 (BioLegend; 144606; 1:100), FITC–anti-Ly6G (BioLegend; 127606; 1:100), APC-Cy7–anti-CD11b (BioLegend; 101226; 1:100) and AF647–anti-Siglec-F (BD Biosciences; 562680; 1:100). Dead cells were detected by using 7-AAD (BioLegend; 420404; 1:100) and excluded from the analysis.

To stain intracellular cytokines, isolated lung cells were cultured in RPMI-1640 complete medium supplemented with 10% (vol/vol) heat-inactivated fetal bovine serum (Thermo Fisher Scientific), 50 U ml^{-1} penicillin + 50 μg ml^{-1} streptomycin (Nacalai Tesque), 55 μM 2-mercaptoethanol (Nacalai Tesque) and 1 mM sodium pyruvate (Nacalai Tesque) in the presence of 20 ng ml^{-1} phorbol 12-myristate 13-acetate (Sigma-Aldrich), 1 μg ml^{-1} ionomycin (Sigma-Aldrich) and brefeldin A (BioLegend) at 37°C for 6 h in an incubation chamber. Then, dead cells were excluded from the analysis by using Zombie-NIR Fixable Viability Kit (BioLegend; 423106; 1:100). Samples were then stained with an anti-CD16/32 monoclonal antibody followed by staining with the following fluorescently labeled monoclonal antibodies against cell surface molecules: BV421–anti-TCRβ (BioLegend; 109230; 1:100) and peridinin chlorophyll protein complex–anti-CD4 (BioLegend; 100432; 1:100). After fixation and permeabilization by using a Cytofix/Cytoperm Fixation/Permeabilization Kit (BD Biosciences) in accordance with the manufacturer's protocol, cells were stained with AF647–anti-IL-17A (BioLegend; 560184; 1:100) and phycoerythrin–anti-IFNγ (BioLegend; 505808; 1:100). Samples were examined by using a FACSAria cell sorter (BD Biosciences), and data analysis was performed by using FlowJo 9.9 software (Tree Star, Ashland, OR, USA).

IFNγ ELIspot

IFNγ ELIspot assay was performed by using a Murine IFNγ Single-color Enzymatic ELIspot Assay Kit (Cellular

Technology Limited, Cleveland, OH, USA) in accordance with the manufacturer's instructions. Freshly isolated lung cells ($0.5–1.0 \times 10^5$ per well) were incubated in CTL-Test Medium (Cellular Technology Limited) containing 2 mM glutamine (Medical & Biological Laboratories, Nagoya, Japan) and 10 μg ml^{-1} peptide-25, an I-A^b-restricted CD4 epitope of Ag85B protein (aa240–254) (29) (Sequence; FQDAYNAAGGHNAVF; GenScript, Tokyo, Japan) overnight at 37°C in a 5% CO_2 atmosphere in an incubation chamber (Cosmo Bio). The number of spot-forming cells was determined by using a CTL S6 Analyzer, ImmunoSpot software (version 5.0) and Immuno Capture software (version 6.3) (Cellular Technology Limited).

Enzyme-linked immunosorbent assay

Enzyme-linked immunosorbent assay (ELISA) was performed as described previously with modifications (30). Two weeks after the final immunization, bronchoalveolar lavage fluid (BALF) was obtained for analysis by means of ELISA. Nunc MaxiSorp flat-bottom 96-well plates (Thermo Fisher Scientific) were coated with Ag85B (1 μg per well) overnight at 4°C. The plates were then washed three times with 0.1% (vol/vol) Tween-20 (Nacalai Tesque) in PBS and blocked with 1% (wt/vol) bovine serum albumin (Nacalai Tesque) in PBS for 1 h at room temperature, followed by washing three times with 0.1% (vol/vol) Tween-20 in PBS. Feces or serum samples, serially diluted with PBS containing 1% (wt/vol) bovine serum albumin, were applied to the plates and incubated for 3 h at 4°C, and then washed three times with 0.1% (vol/vol) Tween-20 in PBS. The plates were then incubated with anti-mouse IgA-horseradish peroxidase (Southern Biotech, Birmingham, AL, USA; SBA-1040-05-1; 1:4000) in 2% (vol/vol) bovine serum albumin and 0.1% (vol/vol) Tween-20 in PBS for 30 min at room temperature, followed by washing three times with 0.1% (vol/vol) Tween-20 in PBS. Antigen-specific antibody titers were visualized by adding TMB microwell peroxidase substrate (SeraCare Life Sciences, Milford, MA, USA) to the wells for 20 min at room temperature in the dark. Then, 0.5 M HCl (Nacalai Tesque) was added to the samples, and absorbance at an optical density of 450 nm was measured by using an iMark microplate reader (Bio-Rad, Hercules, CA, USA).

Bone marrow transplantation

Bone marrow cells were isolated from the femur and tibia of CD11b-DTR transgenic mice (age, 5–8 weeks). Recipient C57BL/6 wild-type mice (age, 5 weeks) were X-irradiated (dose, 8 Gy; MBR-1520R-3, Hitachi, Tokyo, Japan) 6 h before injection of bone marrow cells (1×10^7 per recipient) into the tail vein. Transplanted recipient mice were allowed to recover for at least 8 weeks before being used in the experiments.

Results

iBALT organogenesis is induced by intra-nasal administration of Ag85B-rHPIV2

We first investigated whether intra-nasal administration of Ag85B-rHPIV2 induced iBALT organogenesis. Histological analysis revealed that immunization with Ag85B-rHPIV2 induced the formation of $B220^+$ B-cell follicles, which were absent in PBS-treated control lungs (Fig. 1A). Furthermore, we found that these B-cell follicles were surrounded by $CD3\varepsilon^+$ T cells and $CD11c^+$ DCs, creating a highly organized lymphoid structure (Fig. 1B). In addition, the B-cell follicles contained PNA^+ B cells, suggesting that the germinal center reaction had occurred inside the follicles (Fig. 1B). We also found that the numbers of neutrophils and eosinophils were increased within 48 h after the final immunization. However, the number of those inflammatory cells decreased to the basal level within 2 weeks after the final immunization (Fig. 2). These results indicate that intra-nasal administration with Ag85B-rHPIV2 induced iBALT organogenesis without long-lasting inflammation.

HPIV2 not expressing Ag85B induces iBALT organogenesis

Because Ag85B induces strong T_h1 and T_h17 immune responses (31, 32), we next examined whether iBALT can develop in the absence of Ag85B expression (i.e. administration of null-HPIV2 vector). Immunization with null-HPIV2 vector induced the formation of $B220^+$ B-cell follicles, whereas administration of PBS did not (Fig. 3A). In addition, the B-cell follicles possessed a highly organized lymphoid structure that included B cell and T cell–DC areas (Fig. 3B). $CD11b^+CD11c^+$ DCs were frequently observed in these T cell–DC areas (Fig. 3B). Flow cytometric analysis revealed that the number of T_h17 cells was increased in the lung of mice administered null-HPIV2 vector compared with in the lung of mice administered PBS (Fig. 3C). The numbers of T_h1 cells were not different between mice administered null-HPIV2 vector and those administered PBS (Fig. 3C). These results indicate that nasal immunization with null-HPIV2 vector was sufficient to induce iBALT organogenesis by inducing $CD11b^+CD11c^+$ DCs and T_h17 cells, suggesting its potential as an iBALT organogenesis-inducing vector for respiratory vaccination.

iBALT contributes to the induction of antigen-specific immune responses by Ag85B-rHPIV2

Given that Ag85B-rHPIV2 induces iBALT organogenesis, we next examined the contribution of iBALT to the antigen-specific immune response in the lung by treating cells with LTβR-Fc fusion protein to neutralize the lymphotoxin pathway and disrupt the iBALT structure (18).

After immunization with Ag85B-rHPIV2, flow cytometric analysis revealed that the proportion of $GL7^+$ germinal center B cells was increased among the B-cell population in the lung, which was reversed by LTβR-Fc treatment (Fig. 4A). Consistent with these findings, histological analysis revealed that the number of iBALT structures was decreased by LTβR-Fc treatment in mice administered Ag85B-rHPIV2 (Fig. 4B), and the numbers of iBALT structures were correlated with the numbers of Ag85B-specific IFNγ-producing cells (Fig. 4C). Furthermore, the amount of Ag85B-specific IgA in BALF and IgG in serum was significantly decreased by LTβR-Fc treatment in mice administered Ag85B-rHPIV2 (Fig. 4D). We also found that the amount of Ag85B-specific IgG in BALF showed a tendency to be reduced by LTβR-Fc treatment in mice administered Ag85B-rHPIV2 (Fig. 4D). Reduction level of antibody amount was estimated to 1/4, 1/2 and 1/4 in Ag85B-specific IgA and IgG antibodies in BALF,

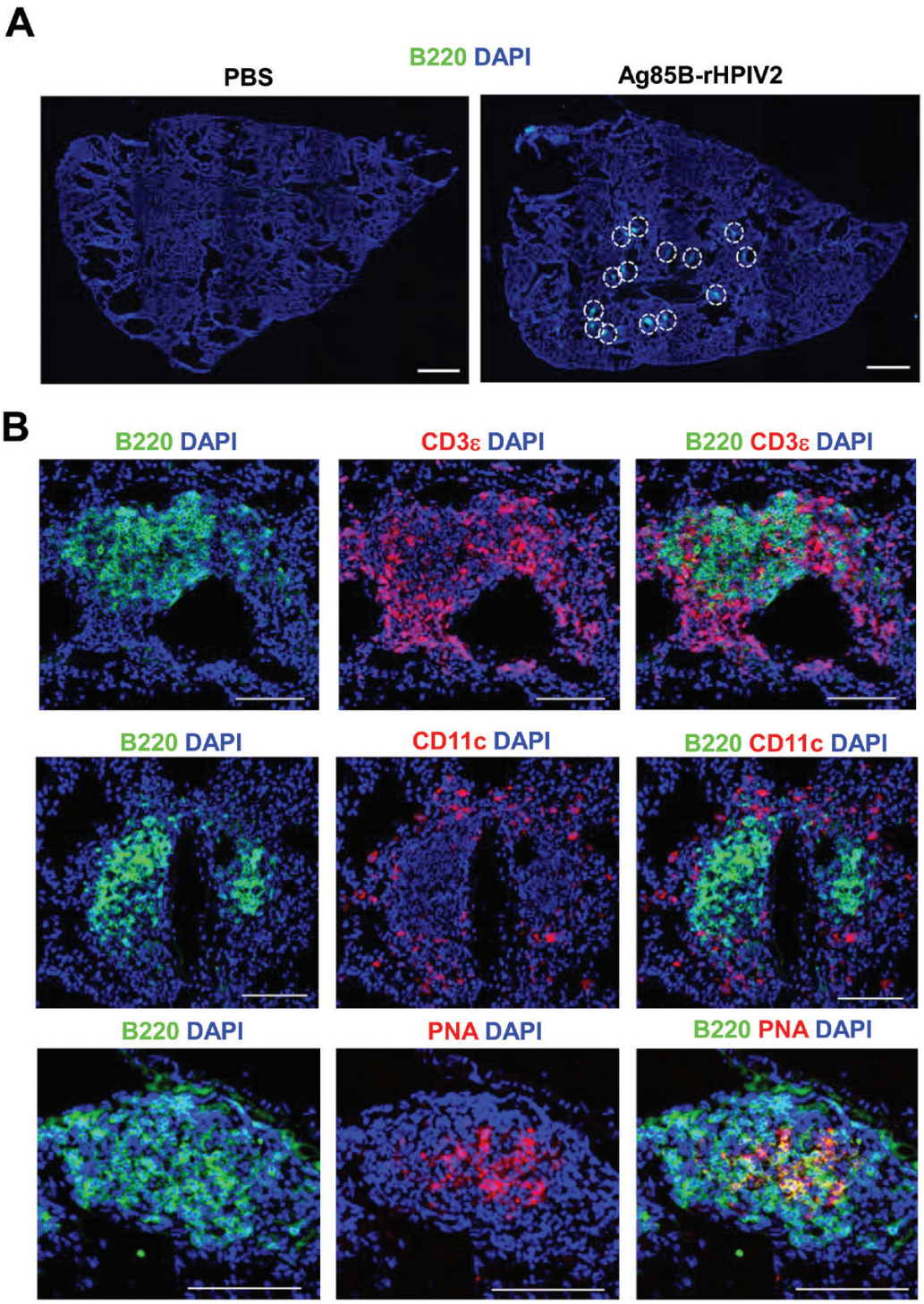

Fig. 1. Intra-nasal administration of Ag85B-rHPIV2 induces iBALT formation. (A, B) Mice were intra-nasally immunized with Ag85B-rHPIV2 four times at 2-week intervals. Two weeks after the final immunization, lung tissues were prepared, stained with the indicated antibodies and reagent, and then examined by means of fluorescence microscopy. Data are representative of four independent experiments. Scale bars: 1 mm (A) and 100 μm (B). Dotted circles in (A) indicate individual iBALT structures.

and IgG antibody in serum, respectively, which were evaluated by sample dilution points and OD450.

To further confirm the role of iBALT in the antigen-specific immune response to Ag85B-rHPIV2, we disrupted the iBALT structure by depleting $CD11b^+$ cells, including $CD11b^+CD11c^+$ DCs, which play important roles in the induction of iBALT organogenesis (5, 18). We used CD11b-DTR transgenic mice and generated CD11b-DTR bone marrow chimeric mice for the sake of repeated injection with diphtheria toxin to deplete $CD11b^+$ cells during the immunization

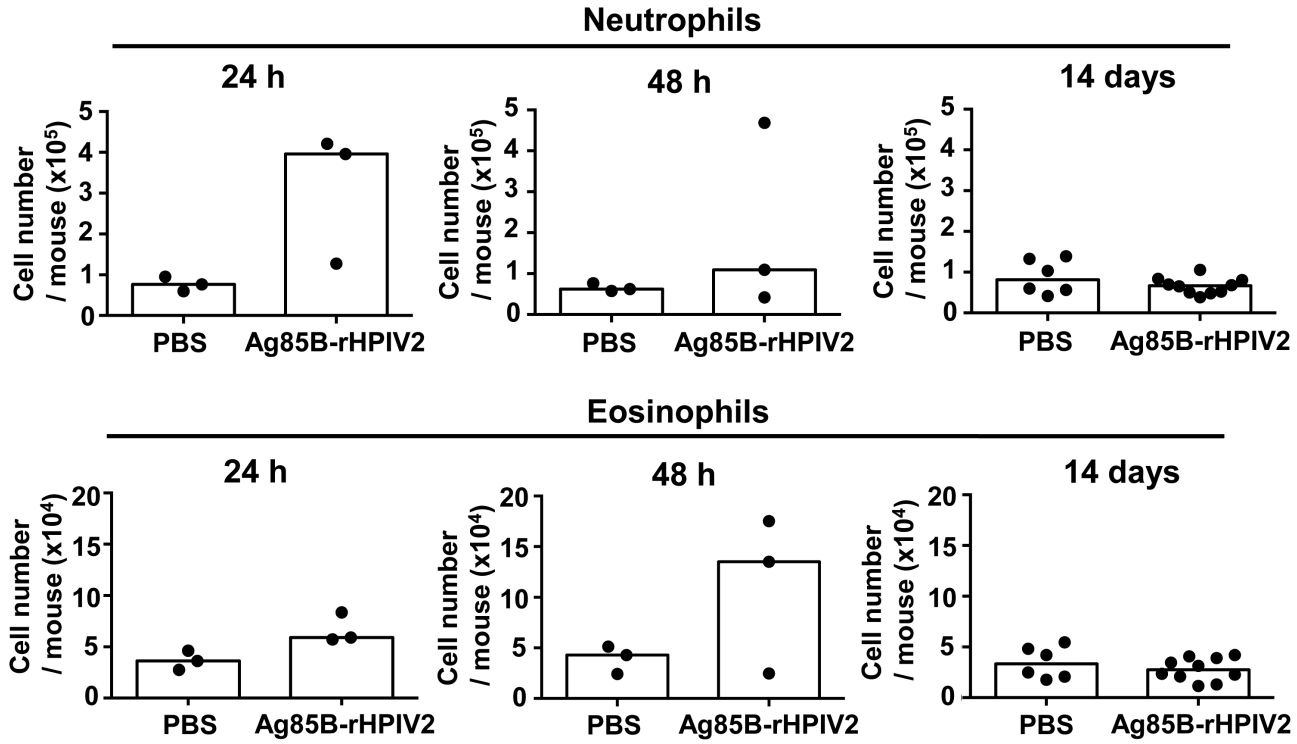

Fig. 2. Intra-nasal administration of Ag85B-rHPIV2 induces temporal inflammatory cell infiltration in the lung. Mice were intra-nasally immunized with Ag85B-rHPIV2 four times at 2-week intervals. Lung cells were isolated and the numbers of neutrophils and eosinophils were examined either at 24 h, 48 h or 2 weeks after the final immunization. Cell number was calculated on the basis of total cell numbers and flow cytometric data. Data are combined from two independent experiments, and each point represents data from an individual mouse. Horizontal lines indicate medians.

period. When bone marrow chimeric mice were administered Ag85B-rHPIV2, the number of iBALT structures was increased compared with control (Fig. 5A), but this increase was inhibited in mice administered both Ag85B-rHPIV2 and diphtheria toxin (Fig. 5A). We also found that, compared with control, the number of Ag85B-specific IFNγ-producing cells in the lung was increased in mice administered Ag85B-rHPIV2 but that this increase was inhibited in mice administered both Ag85B-rHPIV2 and diphtheria toxin (Fig. 5B).

We next examined whether the early phase of immunization is enough to induce Ag85B-specific immune responses in the lung. We immunized mice either two times only at the early phase of the vaccination period (i.e. day 0 and 7) or four times as a conventional vaccination method (day 0, 14, 28 and 42) (Fig. 6A). We found that nasal immunization with Ag85B-rHPIV2 at day 0 induced small and immature iBALT structures without germinal center formation at day 9 (Fig. 6B). Therefore, it is suggested that the early phase of immunization only at day 0 and 7 might be reflecting iBALT-independent immune reactions. We found that Ag85B-specific IFNγ-producing cells and BALF-IgA was not generated when mice were immunized only at the early phase (Fig. 6C and D). These results indicate that Ag85B-specific immune responses, especially respiratory IFN γ-producing T cells and IgA antibody, plausibly depend on the presence of iBALT.

Discussion

BCG is the only currently licensed tuberculosis vaccine. Several lines of evidence have revealed that vaccination with BCG sometimes does not provoke sufficient immune responses, especially against adult pulmonary tuberculosis (20–22). One reason for this insufficient induction of a mucosal immune response may be because BCG is administered via subcutaneous injection. Because the respiratory mucosa is the site of infection by respiratory pathogens, the induction of immune responses in the lung is likely a key factor for the effectiveness of anti-tuberculosis vaccines. It is indicated that mucosal vaccines need adjuvants and targeted delivery systems to overcome mucosal tolerance (33). HPIV2 is a respiratory virus that infects respiratory epithelial cells and potentially induces DC maturation (27, 34). We observed in the present study that intra-nasal inoculation with HPIV2 induced T_h17 cells and $CD11b^+CD11c^+$ DCs in the lung, which led to iBALT organogenesis. Therefore, nasally administered Ag85B-rHPIV2 is a promising novel vaccine against tuberculosis.

In the present study, we found that organogenesis of iBALT contributed to the induction of Ag85B-specific immune responses, such as IFNγ and IgA antibody production in the lung, both of which are likely to be important arms of the protection against tuberculosis (35–37). iBALT organogenesis was induced by inoculation with null-HPIV2 vector, without the expression of Ag85B. It is reported that HPIV2 vector has the ability to induce DC maturation and to increase the expression of MHCI, MHCII, CD86 and cytokines such as IL-6 and IL-12 *in vitro* (34). Our *in vivo* experiment also showed that nasal inoculation of null-HPIV2 vector induced $CD11b^+CD11c^+$ DCs and T_h17 cells in the lung, which are immune cell populations that play critical roles in iBALT organogenesis (5, 6, 18). It is

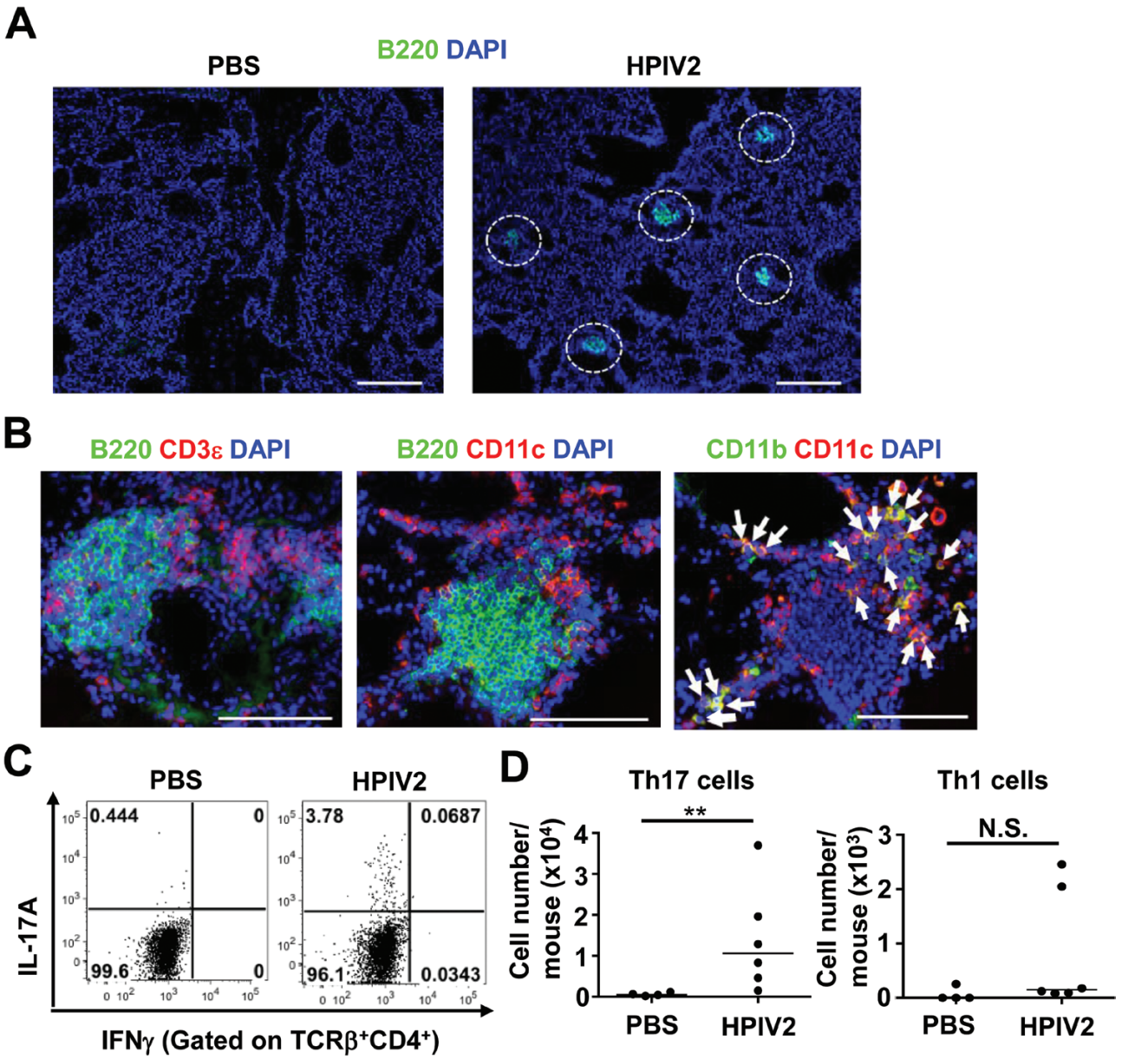

Fig. 3. Ag85B is not essential for the induction of iBALT organogenesis by HPIV2. (A–D) Mice were intra-nasally administered HPIV2, two times at a 1-week interval. Seventeen days after the final immunization, lung samples were examined by means of immunohistochemistry (A, B) and flow cytometry (C, D). (A, B) Lung tissues were prepared and stained with the indicated antibodies and reagent. Data are representative of two independent experiments. Scale bars: 300 μm (A) and 100 μm (B). Dotted circles in (A) indicate individual iBALT structures. Arrows in (B) indicate $CD11b^+CD11c^+$ cells. (C) Representative flow cytometric data of the lung inoculated with either HPIV2 or PBS as a control for the evaluation of cytokine production. $Zombie^-TCR\beta^+CD4^+$ populations are shown. (D) Numbers of T_h17 (gated on $Zombie^-TCR\beta^+CD4^+IL\text{-}17A^+$) and T_h1 (gated on $Zombie^-TCR\beta^+CD4^+IFN\gamma^+$) cells in the lung were determined on the basis of total cell numbers and flow cytometric data. Data are combined from two independent experiments, and each point represents data from an individual mouse. Horizontal lines indicate medians. Statistical significance was evaluated by using the Mann–Whitney test; $^{**}P < 0.01$; N.S., not significant.

worth noting that the T_h1 response was induced in the lung by nasal immunization with Ag85B-rHPIV2 but not by null-HPIV2 vector, suggesting that the HPIV2 vector induced iBALT organogenesis by inducing iBALT inducer cells in an early phase of immunization, and then the Ag85B-specific T_h1 cell response and IgA antibody production were induced inside the iBALT during a later phase of immunization. Indeed, when mice were immunized with Ag85B-rHPIV2 only at the early phase of the immunization period when mature iBALT had not developed yet, Ag85B-specific immune responses were found to be absent, suggesting that presence of iBALT contributes to the induction of Ag85B-specific acquired immune responses.

Previous studies using CD11c-DTR transgenic mice revealed that $CD11b^+CD11c^+$ DCs play an important role in the induction and maintenance of the iBALT structure (5, 18). In the present study, we addressed the issue of iBALT organogenesis by using CD11b-DTR mice and showed

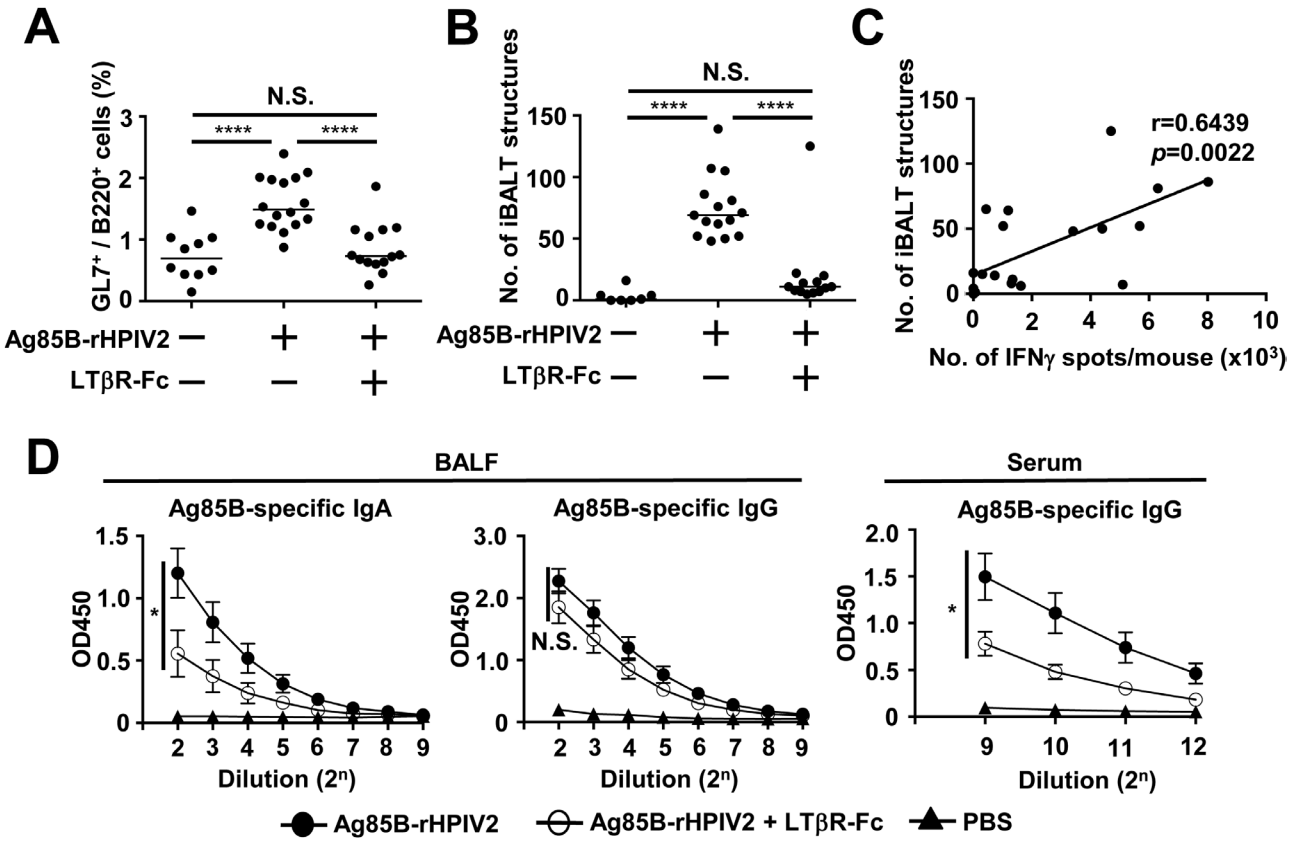

Fig. 4. Lymphotoxin signals are essential for iBALT organogenesis and Ag85B-specific immune responses in the lung. Mice were intra-nasally administered Ag85B-rHPIV2 four times at 2-week intervals with or without LTβR-Fc administration. Lung samples were analyzed 2 weeks after the final immunization with Ag85B-rHPIV2. (A) Lung cells were prepared and examined by flow cytometry. The percentage of $GL7^+$ cells in the $B220^+$ B-cell population is shown. Data are combined from four independent experiments, and each point represents data from an individual mouse. (B) Lung tissues were prepared and examined by means of immunohistochemistry. Eight separate slides were prepared from each lung sample for the counting of iBALT structures. Data are combined from four independent experiments, and each point represents data from an individual mouse. In both plots, center values indicate the median. Statistical significance was evaluated by using one-way ANOVA; $^{****}P < 0.0001$; N.S., not significant. (C) Lung cells were prepared and then examined by means of IFNγ ELIspot assay. Pearson's correlation analysis was conducted between the numbers of IFNγ spots and iBALT structures. (D) BALF and serum were prepared and examined by means of an ELISA for the production of Ag85B-specific IgA and IgG antibodies. Data are combined from four independent experiments and expressed as mean ± SEM (n = 10–16 per group). Statistical significance was evaluated by using Student's t-test; $^*P < 0.05$; N.S., not significant.

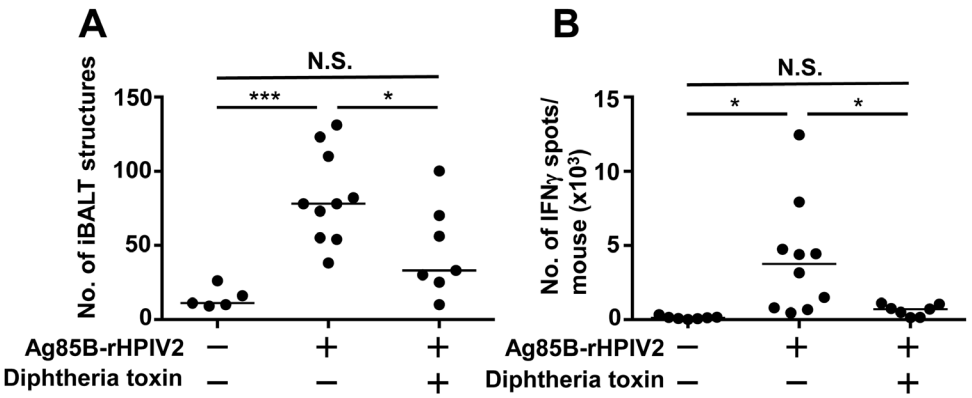

Fig. 5. $CD11b^+$ cells are essential for iBALT organogenesis and Ag85B-specific immune response in the lung. CD11b-DTR bone marrow chimera mice were intra-nasally administered Ag85B-rHPIV2 four times at 2-week intervals with or without diphtheria toxin injection. Lung samples were analyzed 2 weeks after the final immunization with Ag85B-rHPIV2. (A) Lung tissues were prepared and examined by means of immunohistochemistry. Eight separate slides were prepared from each lung sample for the counting of iBALT structures. (B) Lung cells were prepared and then analyzed by means of an IFNγ-ELIspot assay. In both plots, data are combined from four independent experiments and each point represents data from an individual mouse. Center values indicate the median. Statistical significance was evaluated by using one-way ANOVA; $^{***}P < 0.001$; $^*P < 0.05$; N.S., not significant.

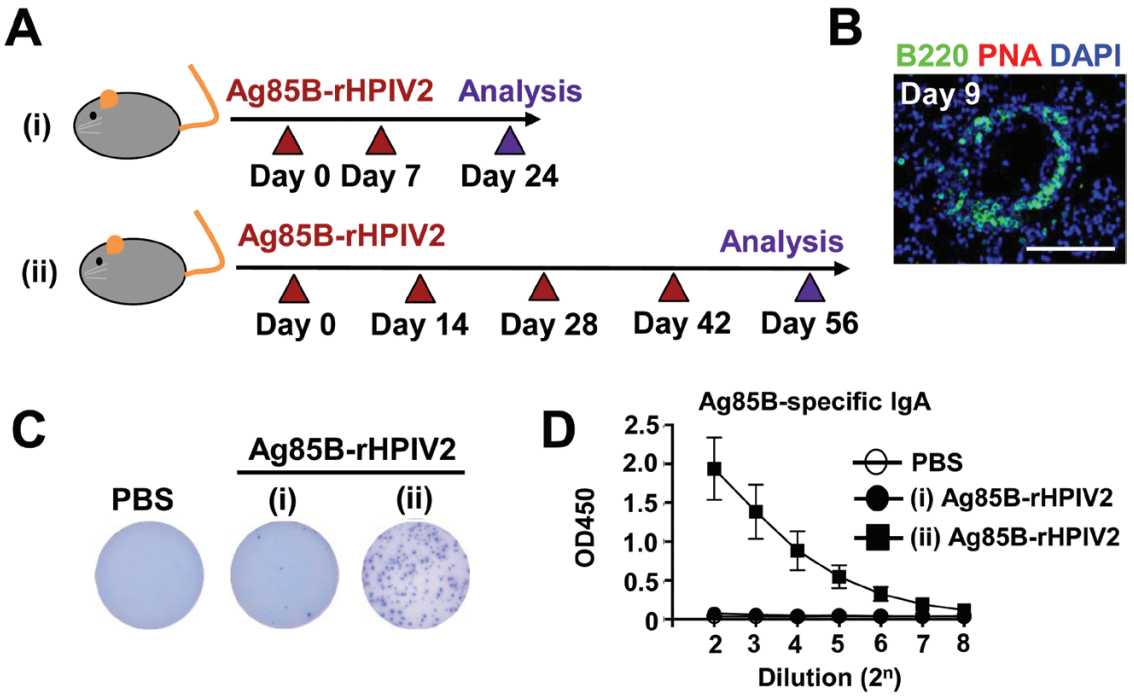

Fig. 6. Ag85B-specific immune response depends on the presence of iBALT. (A) Immunization schedule of Ag85B-rHPIV2. (i) Mice were nasally immunized with Ag85B-rHPIV2, two times only at early phase on day 0 and 7 and examined on day 24. (ii) Mice were nasally immunized with Ag85B-rHPIV2, four times as conventional method on day 0, 14, 28 and 42, and examined on day 56. (B) On day 9, lung tissues were prepared, stained with the indicated antibodies and reagent and then examined by means of fluorescence microscopy. Data are representative of two independent experiments. Scale bars: 100 μm. (C) Lung cells were prepared and then analyzed by means of an IFNγ-ELIspot assay. Data are representative pictures of two independent experiments (n = 4–8 per group). (D) BALF was prepared and examined by means of an ELISA for the production of Ag85B-specific IgA antibody. Data are combined from two independent experiments and expressed as mean ± SEM (n = 4 per group).

that depletion of CD11b$^+$ cells resulted in defective iBALT organogenesis. In addition to CD11b$^+$CD11c$^+$ DCs, CD11b is expressed on interstitial macrophages (38). Also, alveolar macrophages reportedly express CD11b in the state of infection (39). It was reported that alveolar macrophages were involved in the iBALT organogenesis. Indeed, fine particles such as aluminum salts induce iBALT organogenesis via an alveolar macrophage cell death-mediated mechanism (7). It was noteworthy that the alveolar macrophage-initiated iBALT organogenesis was independent from lymphotoxin, but mediated by IL-1α (7) and consequent induction of T_h17 cell differentiation (40, 41), suggesting that alveolar macrophages were unlikely involved in the iBALT organogenesis induced by rHPIV2. Alternatively, several lines of evidence suggest that expression of lymphotoxin was mainly provided by DCs in the process of iBALT organogenesis but not by interstitial and alveolar macrophages (7, 18), implicating that CD11b$^+$CD11c$^+$ DCs are likely to play a major role in Ag85B-rHPIV2-induced iBALT organogenesis as lymphotoxin signals were essential.

In this study, our strategy to investigate the role of iBALT largely depended on the disruption of iBALT structure by neutralizing the lymphotoxin pathway using LTβR-Fc fusion protein or depletion of CD11b$^+$CD11c$^+$ DCs using the CD11b-DTR system. In addition to the effect of these strategies on iBALT development, LTβR-Fc fusion protein reportedly affected the lymphoid structure of the spleen (42, 43), and the CD11b-DTR system reportedly depleted conventional CD11b$^+$ cells, including macrophages (26, 44). Therefore, we cannot rule out the possibility that these multiple effects might have affected the Ag85B-specific immune responses. As there are no iBALT-specific molecular and cellular mechanisms at present, identification of specific developmental mechanism is a key to directly show the evidence of the exact role of iBALT in the respiratory immune system.

Although HPIV2 does not cause respiratory disease in healthy adults, it is a respiratory pathogen responsible for acute respiratory tract illnesses such as common cold, croup, bronchitis, bronchiolitis, hoarseness and pneumonia in children (45–47). Given that BCG contributes substantially to the control of tuberculosis in infants and young children, we suggest that the combination of systemically vaccinating children with BCG and intra-nasally vaccinating adults with Ag85B-rHPIV2 may be a good strategy for increasing community immunity against tuberculosis.

In summary, we demonstrated that an Ag85B-HPIV2-based anti-tuberculosis nasal vaccine induced antigen-specific immune responses in the mouse lung by inducing iBALT organogenesis in a lymphotoxin pathway and CD11b$^+$ cell-dependent manner.

Funding

This work was partially supported by the Japan Agency for Medical Research and Development (AMED) (grant numbers JP17fk0108107h0002 to K.J.I., T.No., Y.Y. and J.K.; JP17ak0101068h0001 to K.I., Y.Y., E.K. and J.K.; JP17fm0208011h 0001 to N.I.) and a Grant-in Aid for Scientific Research from the Ministry of Education, Culture, Sports, Science and Technology (MEXT) and the Japan Society for the Promotion of Science (JSPS)

(MEXT/JSPS KAKENHI grant numbers JP15K19142 to T.Na., JP17K08301 to H.S., and JP24591145 and JP16H05256 to E.K.; JP18J00556 and JP18K17997 to K.H., JP18H02857 to N.I., and JP18H02674 to J.K.).

Acknowledgements

We thank Dr C.F. Ware (Infectious and Inflammatory Diseases Research Center, USA) for providing the plasmid encoding LTβR-Fc. We also thank the laboratory members for their helpful discussions.

Conflicts of interest statement: T.No. has shares of stock in Biocomo Inc. The other authors declared no conflicts of interest.

References

1 Nagatake, T., Fukuyama, S., Kim, D. Y. *et al.* 2009. Id2$^-$, RORγt$^-$, and LTβR-independent initiation of lymphoid organogenesis in ocular immunity. *J. Exp. Med.* 206:2351.
2 Kiyono, H. and Fukuyama, S. 2004. NALT- versus Peyer's-patch-mediated mucosal immunity. *Nat. Rev. Immunol.* 4:699.
3 Hwang, J. Y., Randall, T. D. and Silva-Sanchez, A. 2016. Inducible bronchus-associated lymphoid tissue: taming inflammation in the lung. *Front. Immunol.* 7:258.
4 Moyron-Quiroz, J. E., Rangel-Moreno, J., Kusser, K. *et al.* 2004. Role of inducible bronchus associated lymphoid tissue (iBALT) in respiratory immunity. *Nat. Med.* 10:927.
5 Halle, S., Dujardin, H. C., Bakocevic, N. *et al.* 2009. Induced bronchus-associated lymphoid tissue serves as a general priming site for T cells and is maintained by dendritic cells. *J. Exp. Med.* 206:2593.
6 Rangel-Moreno, J., Carragher, D. M., de la Luz Garcia-Hernandez, M. *et al.* 2011. The development of inducible bronchus-associated lymphoid tissue depends on IL-17. *Nat. Immunol.* 12:639.
7 Kuroda, E., Ozasa, K., Temizoz, B. *et al.* 2016. Inhaled fine particles induce alveolar macrophage death and interleukin-1α release to promote inducible bronchus-associated lymphoid tissue formation. *Immunity* 45:1299.
8 van der Strate, B. W., Postma, D. S., Brandsma, C. A. *et al.* 2006. Cigarette smoke-induced emphysema: a role for the B cell? *Am. J. Respir. Crit. Care Med.* 173:751.
9 Guest, I. C. and Sell, S. 2015. Bronchial lesions of mouse model of asthma are preceded by immune complex vasculitis and induced bronchial associated lymphoid tissue (iBALT). *Lab. Invest.* 95:886.
10 Chvatchko, Y., Kosco-Vilbois, M. H., Herren, S., Lefort, J. and Bonnefoy, J. Y. 1996. Germinal center formation and local immunoglobulin E (IgE) production in the lung after an airway antigenic challenge. *J. Exp. Med.* 184:2353.
11 Elliot, J. G., Jensen, C. M., Mutavdzic, S., Lamb, J. P., Carroll, N. G. and James, A. L. 2004. Aggregations of lymphoid cells in the airways of nonsmokers, smokers, and subjects with asthma. *Am. J. Respir. Crit. Care Med.* 169:712.
12 Hogg, J. C., Chu, F., Utokaparch, S. *et al.* 2004. The nature of small-airway obstruction in chronic obstructive pulmonary disease. *N. Engl. J. Med.* 350:2645.
13 Yokota, Y., Mansouri, A., Mori, S. *et al.* 1999. Development of peripheral lymphoid organs and natural killer cells depends on the helix-loop-helix inhibitor Id2. *Nature* 397:702.
14 Sun, Z., Unutmaz, D., Zou, Y. R. *et al.* 2000. Requirement for RORgamma in thymocyte survival and lymphoid organ development. *Science* 288:2369.
15 Eberl, G., Marmon, S., Sunshine, M. J., Rennert, P. D., Choi, Y. and Littman, D. R. 2004. An essential function for the nuclear receptor RORgamma(t) in the generation of fetal lymphoid tissue inducer cells. *Nat. Immunol.* 5:64.
16 Rangel-Moreno, J., Moyron-Quiroz, J. E., Carragher, D. M. *et al.* 2009. Omental milky spots develop in the absence of lymphoid tissue-inducer cells and support B and T cell responses to peritoneal antigens. *Immunity* 30:731.
17 Rangel-Moreno, J., Moyron-Quiroz, J. E., Hartson, L., Kusser, K. and Randall, T. D. 2007. Pulmonary expression of CXC chemokine ligand 13, CC chemokine ligand 19, and CC chemokine ligand 21 is essential for local immunity to influenza. *Proc. Natl Acad. Sci. USA* 104:10577.
18 GeurtsvanKessel, C. H., Willart, M. A., Bergen, I. M. *et al.* 2009. Dendritic cells are crucial for maintenance of tertiary lymphoid structures in the lung of influenza virus-infected mice. *J. Exp. Med.* 206:2339.
19 Kocks, J. R., Davalos-Misslitz, A. C., Hintzen, G., Ohl, L. and Förster, R. 2007. Regulatory T cells interfere with the development of bronchus-associated lymphoid tissue. *J. Exp. Med.* 204:723.
20 Anonymous.1996. Randomised controlled trial of single BCG, repeated BCG, or combined BCG and killed *Mycobacterium leprae* vaccine for prevention of leprosy and tuberculosis in Malawi. Karonga Prevention Trial Group. *Lancet* 348:17.
21 Rodrigues, L. C., Pereira, S. M., Cunha, S. S. *et al.* 2005. Effect of BCG revaccination on incidence of tuberculosis in school-aged children in Brazil: the BCG-REVAC cluster-randomised trial. *Lancet* 366:1290.
22 Trunz, B. B., Fine, P. and Dye, C. 2006. Effect of BCG vaccination on childhood tuberculous meningitis and miliary tuberculosis worldwide: a meta-analysis and assessment of cost-effectiveness. *Lancet* 367:1173.
23 Belisle, J. T., Vissa, V. D., Sievert, T., Takayama, K., Brennan, P. J. and Besra, G. S. 1997. Role of the major antigen of *Mycobacterium tuberculosis* in cell wall biogenesis. *Science* 276:1420.
24 Watanabe, K., Matsubara, A., Kawano, M. *et al.* 2014. Recombinant Ag85B vaccine by taking advantage of characteristics of human parainfluenza type 2 virus vector showed *Mycobacteria*-specific immune responses by intranasal immunization. *Vaccine* 32:1727.
25 Rooney, I., Butrovich, K. and Ware, C. F. 2000. Expression of lymphotoxins and their receptor-Fc fusion proteins by baculovirus. *Methods Enzymol.* 322:345.
26 Duffield, J. S., Forbes, S. J., Constandinou, C. M. *et al.* 2005. Selective depletion of macrophages reveals distinct, opposing roles during liver injury and repair. *J. Clin. Invest.* 115:56.
27 Kitagawa, H., Kawano, M., Yamanaka, K. *et al.* 2013. Intranasally administered antigen 85B gene vaccine in non-replicating human parainfluenza type 2 virus vector ameliorates mouse atopic dermatitis. *PLoS One* 8:e66614.
28 Nagatake, T., Fukuyama, S., Sato, S. *et al.* 2015. Central role of core binding factor β2 in mucosa-associated lymphoid tissue organogenesis in mouse. *PLoS One* 10:e0127460.
29 Kariyone, A., Tamura, T., Kano, H. *et al.* 2003. Immunogenicity of peptide-25 of Ag85B in T_h1 development: role of IFN-gamma. *Int. Immunol.* 15:1183.
30 Kunisawa, J., Gohda, M., Hashimoto, E. *et al.* 2013. Microbe-dependent CD11b$^+$ IgA$^+$ plasma cells mediate robust early-phase intestinal IgA responses in mice. *Nat. Commun.* 4:1772.
31 Takamura, S., Matsuo, K., Takebe, Y. and Yasutomi, Y. 2005. Ag85B of mycobacteria elicits effective CTL responses through activation of robust T_h1 immunity as a novel adjuvant in DNA vaccine. *J. Immunol.* 175:2541.
32 Tsujimura, Y., Inada, H., Yoneda, M., Fujita, T., Matsuo, K. and Yasutomi, Y. 2014. Effects of mycobacteria major secretion protein, Ag85B, on allergic inflammation in the lung. *PLoS One* 9:e106807.
33 Fujkuyama, Y., Tokuhara, D., Kataoka, K. *et al.* 2012. Novel vaccine development strategies for inducing mucosal immunity. *Expert Rev. Vaccines* 11:367.
34 Hara, K., Fukumura, M., Ohtsuka, J., Kawano, M. and Nosaka, T. 2013. Human parainfluenza virus type 2 vector induces dendritic cell maturation without viral RNA replication/transcription. *Hum. Gene Ther.* 24:683.
35 Zhu, B., Dockrell, H. M., Ottenhoff, T. H. M., Evans, T. G. and Zhang, Y. 2018. Tuberculosis vaccines: opportunities and challenges. *Respirology* 23:359.
36 O'Garra, A., Redford, P. S., McNab, F. W., Bloom, C. I., Wilkinson, R. J. and Berry, M. P. 2013. The immune response in tuberculosis. *Annu. Rev. Immunol.* 31:475.
37 Reljic, R., Williams, A. and Ivanyi, J. 2006. Mucosal immunotherapy of tuberculosis: is there a value in passive IgA? *Tuberculosis (Edinb.)* 86:179.

38 Hussell, T. and Bell, T. J. 2014. Alveolar macrophages: plasticity in a tissue-specific context. *Nat. Rev. Immunol*. 14:81.
39 Cahayani, W. A., Norahmawati, E., Budiarti, N. and Fitri, L. E. 2016. Increased CD11b and hypoxia-inducible factors-1alpha expressions in the lung tissue and surfactant protein-D levels in serum are related with acute lung injury in severe malaria of C57BL/6 mice. *Iran. J. Parasitol*. 11:303.
40 Chung, Y., Chang, S. H., Martinez, G. J. *et al.* 2009. Critical regulation of early T_h17 cell differentiation by interleukin-1 signaling. *Immunity* 30:576.
41 Sutton, C. E., Lalor, S. J., Sweeney, C. M., Brereton, C. F., Lavelle, E. C. and Mills, K. H. 2009. Interleukin-1 and IL-23 induce innate IL-17 production from gammadelta T cells, amplifying T_h17 responses and autoimmunity. *Immunity* 31:331.
42 Rennert, P. D., Browning, J. L., Mebius, R., Mackay, F. and Hochman, P. S. 1996. Surface lymphotoxin alpha/beta complex is required for the development of peripheral lymphoid organs. *J. Exp. Med*. 184:1999.
43 Mackay, F., Majeau, G. R., Lawton, P., Hochman, P. S. and Browning, J. L. 1997. Lymphotoxin but not tumor necrosis factor functions to maintain splenic architecture and humoral responsiveness in adult mice. *Eur. J. Immunol*. 27:2033.
44 Hulsmans, M., Clauss, S., Xiao, L. *et al.* 2017. Macrophages facilitate electrical conduction in the heart. *Cell* 169:510.
45 Wu, K. W., Wang, S. M., Shen, C. F., Ho, T. S., Wang, J. R. and Liu, C. C. 2017. Clinical and epidemiological characteristics of human parainfluenza virus infections of children in southern Taiwan. *J. Microbiol. Immunol. Infect*. doi: 10.1016/j.jmii.2016.08.017.
46 Mizuta, K., Abiko, C., Aoki, Y. *et al.* 2012. Epidemiology of parainfluenza virus types 1, 2 and 3 infections based on virus isolation between 2002 and 2011 in Yamagata, Japan. *Microbiol. Immunol*. 56:855.
47 Weinberg, G. A., Hall, C. B., Iwane, M. K. *et al.*; New Vaccine Surveillance Network. 2009. Parainfluenza virus infection of young children: estimates of the population-based burden of hospitalization. *J. Pediatr*. 154:694.